

# CHARACTERISTICS OF THE CONTRACTION TWINS FORMED IN AZ31 ALLOY DURING TENSILE DEFORMATION

P. Cizek and M.R. Barnett

ITRI, CMFI, Deakin University, Waurn Ponds Vic 3217



## INTRODUCTION

C-axis contraction in magnesium alloys can be accommodated by (10-11)/(10-13) “contraction” twinning and (10-11)/(10-13)-(10-12) double twinning. The formation of contraction twins can cause early shear failure in these alloys due to the combined effects of strain softening of the continuum and localised void formation.

The aim of the present work was to study the contraction twin characteristics in a magnesium polycrystalline alloy, subjected to tensile deformation performed approximately perpendicular to the grain c-axes.

## EXPERIMENTAL

An AZ31 (3wt.%Al-1%Zn) Mg alloy was used in a form of hot rolled plate with fully recrystallised microstructure. The grain c-axes were largely distributed around the plate normal direction. Tensile testing was performed to the point of cracking parallel to the plate rolling direction at room temperature using a strain rate of  $0.01 \text{ s}^{-1}$ . The microstructure was examined using transmission electron microscopy (TEM).

## TWIN/MATRIX MISORIENTATIONS

Major twin/matrix misorientations for the extension twins (E) and single/double contraction twins are summarised below. All six (10-11)-(10-12) double twin variants are shown in **Fig. 1**.

Twin Type	Misorientation Angle/Axis
(10-12) E	$86.3^\circ/[1-210]$
(10-11)	$56.1^\circ/[1-210]$
(10-11)-(10-12) Variant 1	$37.6^\circ/[1-210]$
(10-11)-(10-1-2) Variant 2	$30.1^\circ/[1-210]$
(10-13)	$64.0^\circ/[1-210]$
(10-13)-(10-12) Variant 1	$22.3^\circ/[1-210]$
(10-13)-(10-1-2) Variant 2	$29.8^\circ/[1-210]$

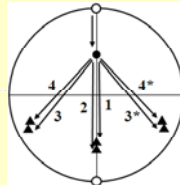


**Figure 1.** (0001) pole figure which shows reorientation of basal poles during (10-11)-(10-12) double twinning. The open circles are the original orientation, the filled circle is the reoriented basal pole after primary (10-11) twinning and the triangles denote the final basal poles after secondary (10-12) twinning; the reorientations for each twinning variant are indicated by the numbers 1–4.

## DOUBLE TWINS

A majority of the observed twins displayed misorientations consistent with the variant 1 of (10-11)-(10-12) double twinning. The variant 2 was only present as small segments embedded in the variant 1 double twins (**Fig. 2**).

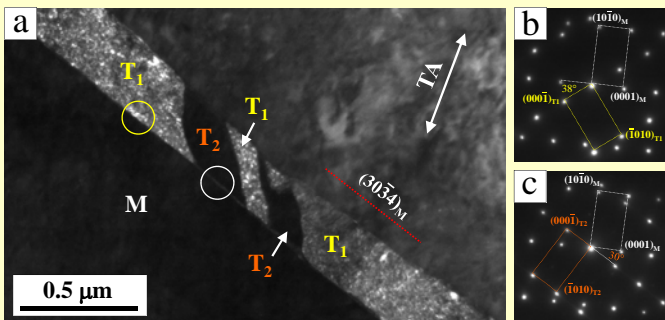


**Figure 2.** TEM analysis of a (10-11)-(10-12) double twin in the matrix M, dominated by type 1 variant  $T_1$  and containing two segments of type 2 variant  $T_2$ . (a) dark-field image in  $(001)_{T_1}$  reflection (TA indicates the tensile axis); (b) SAD pattern from the  $T_1/M$  interface; (c) SAD pattern from the  $T_2/M$  interface. The zone axis vectors in (b) and (c) are  $[1-210]_{T_1/M}$ .

## REASON FOR VARIANT 1 FORMATION

The variant 1 provides the closest match between the primary (10-11) and secondary (10-12) twinning planes and its formation thus allows for the compatibility strain, accompanying growth of the secondary twin within the shape constraints enforced by the primary twin, to be minimized.

## OTHER CONTRACTION TWINS

Some (10-11) twins, or twin segments, with misorientations of about  $56^\circ/[1-210]$  were also present. The (10-13) single twins ( $64^\circ/[1-210]$ ) or (10-13)-(10-12) double twins ( $22^\circ/[1-210]$ ) were found only rarely. It is also occasionally observed that multiple twinning can occur inside the (10-11) contraction twins to establish complex structures comprised of several sequentially formed twin segments (**Fig. 3**).

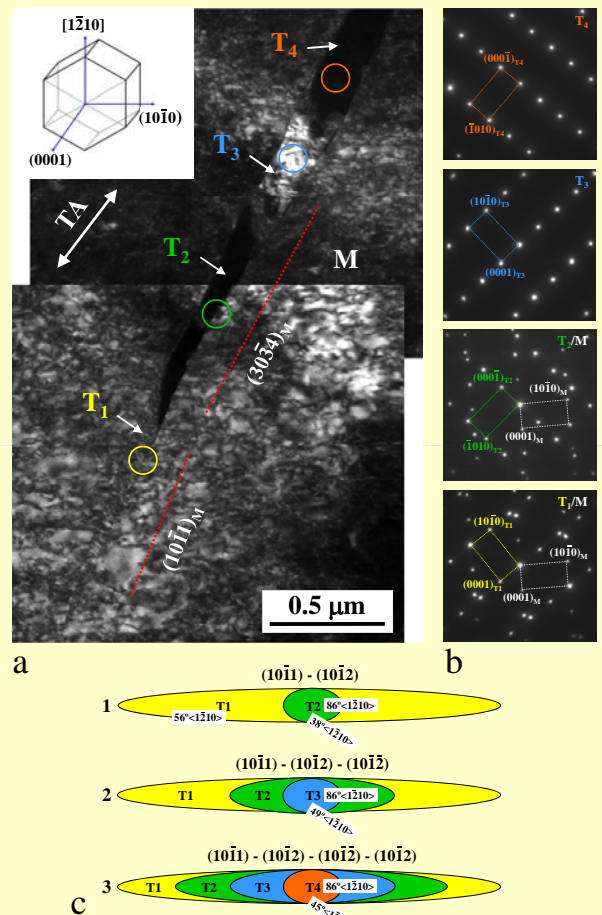


**Figure 3.** (a) TEM dark-field micrograph of a multiple twin formed within the matrix M and composed of segments  $T_1$ - $T_4$ . The  $(10-11)_{T_1/M}$  reflection was used. The insert shows the orientation of the hcp lattice used in the analysis. (b) SAD patterns from the  $T_1$ ,  $T_2$ ,  $T_3$ , and  $T_4$  twin segments, showing the rotation angles of  $56^\circ$ ,  $39^\circ$ ,  $50^\circ$ , and  $45^\circ$ , respectively, relative to M around the common  $[1-210]_{T_1/M}$  axis. The corresponding zone axes are parallel to the  $[1-210]_{T_1/M}$  vectors. (c) Schematic of the twinning sequence 1-3 occurring within the original (10-11) contraction twin and creating the observed segmented twin.

## CONCLUSIONS

It was found that the grain c-axis contractions in the AZ31 Mg alloy deformed in tension to the point of cracking were largely accommodated by the formation of (10-11)-(10-12) double twins in a variant characterized by the  $38^\circ/[1-210]$  twin/matrix misorientation in conjunction with dislocation slip.